

Review

# Functional and Biochemical Analysis of Glucose-6-Phosphate Dehydrogenase (G6PD) Variants: Elucidating the Molecular Basis of G6PD Deficiency

Saúl Gómez-Manzo <sup>1,\*</sup>, Jaime Marcial-Quino <sup>2,\*</sup>, Daniel Ortega-Cuellar <sup>3</sup>, Hugo Serrano-Posada <sup>4</sup>, Abigail González-Valdez <sup>5</sup>, America Vanoye-Carlo <sup>6</sup>, Beatriz Hernández-Ochoa <sup>7</sup>, Edgar Sierra-Palacios <sup>8</sup>, Adriana Castillo-Villanueva <sup>1</sup> and Horacio Reyes-Vivas <sup>1</sup>

- <sup>1</sup> Laboratorio de Bioquímica Genética, Instituto Nacional de Pediatría, Secretaría de Salud, Mexico City 04530, Mexico; acastilloinp@gmail.com (A.C.-V.); hreyesvivas@yahoo.com.mx (H.R.-V.)
  - <sup>2</sup> Consejo Nacional de Ciencia y Tecnología (CONACYT), Instituto Nacional de Pediatría, Secretaría de Salud, Mexico City 04530, Mexico
  - <sup>3</sup> Laboratorio de Nutrición Experimental, Instituto Nacional de Pediatría, Secretaría de Salud, Mexico City 04530, Mexico; dortegadan@gmail.com
  - <sup>4</sup> Consejo Nacional de Ciencia y Tecnología (CONACYT), Laboratorio de Agrobiotecnología, Tecnoparque CLQ, Universidad de Colima, Carretera los Limones-Loma de Juárez, Colima 28629, Mexico; hjserranopo@conacyt.mx
  - <sup>5</sup> Departamento de Biología Molecular y Biotecnología, Instituto de Investigaciones Biomédicas, Universidad Nacional Autónoma de México, Mexico City 04510, Mexico; abigaila@correo.biomedicas.unam.mx
  - <sup>6</sup> Laboratorio de Neurociencias, Instituto Nacional de Pediatría, Secretaría de Salud, Mexico City 04530, Mexico; america\_vc@yahoo.com.mx
  - <sup>7</sup> Laboratorio de Inmunquímica, Hospital Infantil de México Federico Gómez, Mexico City 06720, Mexico; beatrizhb\_16@comunidad.unam.mx
  - <sup>8</sup> Colegio de Ciencias y Humanidades, Plantel Casa Libertad, Universidad Autónoma de la Ciudad de México, Mexico City 09620, Mexico; edgar.sierra@uacm.edu.mx
- \* Correspondance: saulmanzo@ciencias.unam.mx (S.G.-M.); jmarcialqu@conacyt.mx (J.M.-Q.); Tel.: +52-55-1084-0900 (ext. 1442) (S.G.-M. & J.M.-Q.)

Academic Editor: José R. B. Gomes

Received: 10 March 2017; Accepted: 28 April 2017; Published: 2 May 2017

**Abstract:** G6PD deficiency is the most common enzymopathy, leading to alterations in the first step of the pentose phosphate pathway, which interferes with the protection of the erythrocyte against oxidative stress and causes a wide range of clinical symptoms of which hemolysis is one of the most severe. The G6PD deficiency causes several abnormalities that range from asymptomatic individuals to more severe manifestations that can lead to death. Nowadays, only 9.2% of all recognized variants have been related to clinical manifestations. It is important to understand the molecular basis of G6PD deficiency to understand how gene mutations can impact structure, stability, and enzymatic function. In this work, we reviewed and compared the functional and structural data generated through the characterization of 20 G6PD variants using different approaches. These studies showed that severe clinical manifestations of G6PD deficiency were related to mutations that affected the catalytic and structural nicotinamide adenine dinucleotide phosphate (NADPH) binding sites, and suggests that the misfolding or instability of the 3D structure of the protein could compromise the half-life of the protein in the erythrocyte and its activity.

**Keywords:** glucose-6-phosphate dehydrogenase (G6PD); G6PD deficiency; functional and structural characterization; kinetic parameters; computer modelling

## 1. Introduction

The deficiency of glucose-6-phosphate dehydrogenase (G6PD) has been recognized as the most common enzymopathy, affecting nearly 400 million people worldwide [1]. G6PD deficiency is genetically heterogeneous with 217 mutations reported, which have been mainly found in the coding regions and are buried in the enzyme, producing functionally-deficient G6PD variants [2]. This enzymopathy is usually diagnosed and classified through hematological studies and classified based on the level of G6PD enzymatic activity in red blood cells. The G6PD deficiency causes several abnormalities that ranges clinically from asymptomatic individuals through to patients showing neonatal jaundice (NNJ), acute episodes of hemolysis triggered by exogenous agents (acute infections, drugs or food), and chronic nonspherocytic hemolytic anemia (CNSHA) [3]. The difference in severity is due to the different location of mutations in the gene sequence; therefore, it is important to structurally and functionally characterize the altered enzyme to understand the consequences of each mutation.

### 1.1. The Human G6PD Gene

The completed sequence of the human G6PD gene is 18.5 Kb in size and consists of 13 exons and 12 introns encoding a product of 1545 bp [4]. The translated product of this gene is a protein of 515 amino acids with a molecular weight of over 59 kDa [5]. G6PD is a cytosolic protein with a key role in the pentose phosphate pathway (PPP) that produces nicotinamide adenine dinucleotide phosphate (NADPH), a very important reducing agent that confers protection against cellular oxidative stress and helps in the regeneration of oxidized glutathione (GSSG).

The primary and tertiary structure of human G6PD has been determined from the nucleotide sequence of full-length cDNA clones and by crystallographic studies [4,6]. The characterization of the structure showed that the active human G6PD enzyme exists in a dimer or tetramer equilibrium. The dimeric G6PD enzyme has two subunits symmetrically located across a complex interface of  $\beta$ -sheets and each subunit binds to a nicotinamide adenine dinucleotide phosphate (NADP<sup>+</sup>) molecule that confers structural stability. This structural NADP<sup>+</sup> molecule is positioned close to the interface where the two subunits of each dimer are intertwined [7] (Figure 1). In addition, the dimeric form shows an extensive interface region formed by the association of  $\beta + \alpha$  domains located in the C-terminal region of each monomer [8] (Figure 1). The N-terminal domain (amino acids 27–200) contains the  $\beta$ - $\alpha$ - $\beta$  dinucleotide binding site with a Rossmann type folding (amino acids 38–44), where the active site of the enzyme that binds  $\beta$ -D-glucose-6-phosphate (G6P) and NADP<sup>+</sup> is located; and the second binding site consists of an antiparallel nine-strand sheet located near the interface region of the protein known as the “structural NADP<sup>+</sup> binding site” (Figure 1) [7,8]. Interestingly, the second structural NADP<sup>+</sup> binding site is present only in higher organisms and is involved in the dimerization and the stability of the enzyme [6,9]. It is noteworthy that mutations occurring near the structural binding site of NADP<sup>+</sup> decrease the stability of the enzyme, causing severe phenotypes such as CNSHA [10].

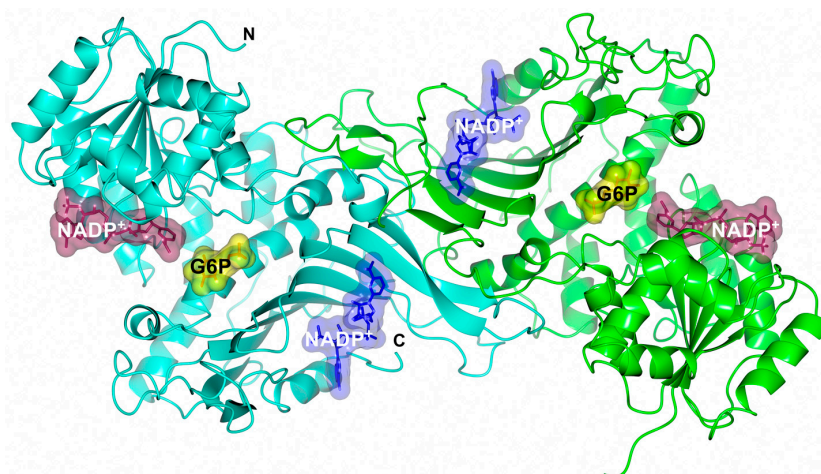


**Figure 1.** Dimeric arrangement of human G6PD enzyme (PDB entries 2BHL and 2BH9). Monomers are drawn in cyan and green. The structural NADP<sup>+</sup>, catalytic NADP<sup>+</sup> and G6P substrate are shown as blue, dark purple and yellow molecular surface representations, respectively. All figures were prepared with CCP4mg (Didcot, UK) [11] using the same color code.

The multiple alignment analysis of more than 100 sequences of G6PD from different organisms was performed and showed a level of identity varying from 30% to 94% [8]. Kotaka and coworkers [8] identified three highly conserved sequences in this multiple alignment: the first is comprised of a 9-residue peptide **RIDHYLGKE** (residues 198–206 single-letter amino acid code of the human G6PD) where Lysine 205 (Lys205) is the amino acid responsible for substrate binding and catalysis in the human G6PD enzyme [12]. A second sequence, a conserved nucleotide-binding fingerprint (**GxxGGDLA**) that has been associated with NADP<sup>+</sup> coenzyme binding is located from amino acids 38–44 in the N-terminal and is encoded by the exon 3 [7]. Finally, the third sequence **EKPxG** (residues 170–174 of human enzyme) containing a Proline 172 (Pro172) is critical for the correct positioning of the substrate (G6P) and coenzyme (NADP<sup>+</sup>) during enzymatic reaction [8]. Interestingly, genetic analysis indicates a high correlation between the degree of conservation of mutated amino acids and the clinical manifestations of the related disease. The more aggressive disease results when the mutations occur either in conserved amino acids, or those that are clustered on exon 10, since the latter encode a segment of the interface region involved in forming the dimeric structure of G6PD enzyme [13].

To understand the molecular basis of G6PD deficiency, it is important to understand how gene mutations impact structure, stability and enzymatic function. Until now, only 9.2% of all recognized variants have been related to clinical manifestations. In this work, we reviewed and compared structural and functional data obtained from the G6PD variants characterized in different reports. We first reviewed the methodological procedures that had been employed and their considerations. Table 1 shows the most relevant information about the characterization of the G6PD variants that have been studied.

**Table 1.** Main data about G6PD variants characterization previously reported.

Mutation Name	cDNA Nucleotide Substitution	Codon	Amino Acid Substitution	Exon	Class	Country of Origin	Reference
Taipei	493A > G	165	Asn → Asp	6	I	China	[14]
Volendam	514C > T	172	Pro → Ser	6	I	Holland	[15]
Andalus	1361G > A	454	Arg → His	11	I	Spain	[16]
Wisconsin	1177C > G	393	Arg → Gly	10	I	USA	[17]
Nashville	1178G > A	393	Arg → His	10	I	USA, Italy, Portugal	[17]
Plymouth	488G > A	163	Gly → Asp	6	I	GB	[18]
Yucatan	1285A > G	429	Lys → Gly	10	I	México	[19]
Durham	713A > G	238	Lys → Arg	7	I	USA	[20]

Table 1. Cont.

Mutation Name	cDNA Nucleotide Substitution	Codon	Amino Acid Substitution	Exon	Class	Country of Origin	Reference
Zacatecas	770G > T	257	Arg → Leu	7	I	México	[21]
Coimbra	592C > T	198	Arg → Cys	6	II	India	[14]
Union	1360C > T	454	Arg → Cys	11	II	Italy, Spain, China, Japan	[16]
Valladolid	406C > T	136	Arg → Cys	5	II	Spain	[19]
Santa-Maria	376A > G	126	Asn → Asp	5, 6	II	Costa Rica, Italy	[20]
A+	542A > T	181	Asp → Val				
	376A > G	126	Asn → Asp	5	III	Africa	[20]
Vanua-Lava	383T > C	128	Leu → Pro	5	II	Southwestern Pacific	[21]
Viangchan	871G > A	291	Val → Met	9	II	China	[21,22]
Mexico City	680G > A	227	Arg → Gln	7	III	México	[19]
Mahidol	487G > A	163	Gly → Ser	6	II	South East Asia	[14,18,22]
Viangchan + Mahidol	871G > A	291	Val → Met	9, 6	II/III	Thailand	[22]
	487G > A	163	Gly → Ser				
	202G > A	68	Val → Met				
A <sup>-</sup>	376A > G	126	Asn → Asp	4,5	III	Africa	[23]

## 1.2. Methodological Approaches for G6PD Expression

### 1.2.1. Construction of Expression Plasmid

Several systems have been implemented to achieve expression and purification of both the wild-type (WT) and G6PD variants. Heterologous expression of human G6PD based on *Escherichia coli* strains and compatible plasmids have been widely used to produce high protein quantities for structural and functional studies [12,14,16,17,19–21,23–26]. During the first characterization studies, the G6PD gene was widely fused to different expression vectors such as pKK223-3, pKK233-2, pMPM-A4Ω and pPLcmu299 [15]. However, these plasmids were discontinued and are no longer commercially available [26].

To overcome this disadvantage, Tang et al. [14] sub-cloned the normal and mutated G6PD gene into a pGEX-3X vector, which allowed the production of a functional glutathione-S-transferase (GST)/G6PD fusion protein in *Escherichia coli*; and observed that the values of kinetic parameters from the biochemical characterization of the resulting proteins were the same as those reported using the initial vectors. These results revealed that this new system was very useful for the expression of normal and mutant enzymes. Subsequently, pTrc99A [16,18,25] was chosen as the expression vector; however, it was not compatible with commercial *E. coli* strains.

Another disadvantage in the use of bacteria expression systems is the low soluble fraction of G6PD. It is caused by an insoluble product that is produced in large amounts relative to the soluble protein [24]. Huang et al. [18] successfully used two strategies to overcome this problem: the co-expression of G6PD Plymouth and Mahidol variants with molecular chaperones as GroEL and GroES; and the growth of *E. coli* at lower temperatures. They observed that both strategies significantly increased the soluble expression of recombinant G6PD Plymouth and Mahidol variants. Other successful expression vectors such as pET30b and peT3a were also frequently employed to produce large quantities of G6PD variants [9,19–21,27]. More recently, the WT G6PD protein was purified using His-tagged systems such as the pET-HisTEVP vector containing the His-tag and a tobacco etch virus protease (TEVP) recognition site at the N-terminal of the protein [26], and the pET28a His-tag [22] containing the His-tag in the N-terminal where the additional His-tag does not affect the catalysis, structure or stability of the WT G6PD enzyme [22,26], making these systems a good option for obtaining sufficient protein for structural and functional studies of human G6PD and its variants. In Table 2, the kinetic properties of recombinant human WT G6PD obtained under diverse expression systems are summarized, highlighting that no significant changes were observed between the vector systems, thus suggesting that all described approaches could be useful in G6PD studies.

**Table 2.** Kinetic constants for recombinant human wild-type (WT) G6PDs and values of reported kinetic properties for human recombinant G6PD using different expression vectors.

Plasmid Expression	$K_m$ G6P ( $\mu\text{M}$ )	$K_m$ NADP <sup>+</sup> ( $\mu\text{M}$ )	$k_{\text{cat}}$ ( $\text{s}^{-1}$ )	$k_{\text{cat}}/K_m$ G6P ( $\text{s}^{-1}/\mu\text{M}$ )	$k_{\text{cat}}/K_m$ NADP <sup>+</sup> ( $\text{s}^{-1}/\mu\text{M}$ )	Reference
pKK233-2	69	12	220	n.d.	n.d.	[24]
pMPM-A4 $\Omega$	65	12	210	n.d.	n.d.	[15]
pPLcmu299	72	13	180	$3.18 \times 10^6$	$13.84 \times 10^6$	[24]
pGEX-3X	48	8	n.d.	n.d.	n.d.	[14]
pTrc	52	7.07	275	$5.31 \times 10^6$	$39.7 \times 10^6$	[16]
pTrc99A	45.8	4.6	251	$5.48 \times 10^6$	$53.7 \times 10^6$	[25]
pET30b	52	7.07	275	$5.31 \times 10^6$	$39.7 \times 10^6$	[17,28]
pTrc99A	54.8	6.7	161	$2.94 \times 10^6$	$24.03 \times 10^6$	[18]
pET-HisTEVP	65	15	282	$4.33 \times 10^6$	$18.8 \times 10^6$	[26]
peT3a	38.49	6.16	233	$6.05 \times 10^6$	$37.82 \times 10^6$	[19–21]
pET28a His-tag	47.8	7.2	247	$5.2 \times 10^6$	$34.3 \times 10^6$	[22]

n.d = not determined.

### 1.2.2. *E. coli* G6PD-Deficient Strains

Another useful tool for G6PD human expression is through genetically modified *E. coli* strains. This system has allowed for easier and more precise characterization of pure recombinant G6PD enzymes as the endogenous G6PD enzyme is deleted. The *E. coli* strain HB351 ( $\Delta(\text{lac}), \Delta(\text{zwf-Edd})\text{-Zeb::Tn10}$ ), is one of the first strains used for this purpose [24]; however, another *E. coli* DR612 strain that lacks endogenous G6PD, has also been used to express a Volendam mutation [15]. Finally, Gomez-Manzo et al. [19] also generated a G6PD knock-out of the *E. coli* BL21 (DE3)  $\Delta\text{zwf}::\text{kanr}$  strain, via genetic recombination and mediated by P1vir transduction. This strain was used to express G6PD mutants Yucatan, Valladolid, Mexico City, Nashville, Durham, Santa-Maria, A+, Zacatecas, Viangchan and Vanua-Lava. Recently, Boonyuen et al. [22] used the pET28a expression vector with an N-terminal His-tag in an expression BL21 (DE3) cell.

### 1.2.3. Optimization of G6PD Expression

In general, the use of bacterial expression systems for recombinant proteins has become one of the most common strategies for producing proteins on a large scale; however, it is noteworthy that several issues should be overcome before producing soluble and correctly folded recombinant proteins [24]. One way to assess the optimal expression level of G6PD is through the measurement of its specific activity from crude extracts obtained using an expression system. A common strategy to attain large quantities of soluble recombinant human G6PD protein is to decrease the growth temperature as well as modify the isopropyl- $\beta$ -D-thiogalactopyranoside (IPTG) concentration. At low temperatures, the recombinant protein can reach a proper folding. Several groups have performed the expression of both WT and mutants of G6PD at different temperatures from 15 to 37 °C [14–21,24,25]. Specifically, Gómez-Manzo et al. [19–21], found that soluble G6PD levels were highest at 25 °C for the G6PD Yucatan, Valladolid, Mexico City, Nashville, Durham, Santa-Maria, A+, Zacatecas, Viangchan and Vanua-Lava variants. Furthermore, they also found that the optimal G6PD expression was time (18 h) and isopropyl- $\beta$ -D-thiogalactopyranoside (IPTG) concentration dependent; however, the use of these conditions does not avoid the formation of inactive inclusion bodies [19–21]. On the other hand, Boonyuen et al. [22] expressed G6PD Mahidol and Viangchan variants at 20 °C, inducing with 1 mM IPTG at 20 h, while the G6PD Plymouth and Mahidol were expressed at 37 °C for 24 h IPTG induction [18]. Furthermore, the G6PD Unión and Andalus variants were grown at 37 °C [16] and the clinical Wisconsin and Nashville variants were allowed to grow for another 5 h at 30 °C. Finally, the G6PD Volendam expression was obtained using 2% of arabinose as an inducer [15]. The vector selection and optimization of the culture conditions are crucial steps for the optimal expression level of G6PD. It has been observed that if an unsuitable vector is chosen, only 0.5 mg of product per liter of culture is obtained; conversely, a proper choice can lead to an average production of 3–5 mg/L, reaching the best conditions up to 25 mg per liter of culture [12,14,16–21,24,25].

In almost all cases, the purification process of the protein has been conducted with affinity chromatography with 2′5′ADP Sepharose 4B (an NADP<sup>+</sup> structural analog) [12,14,16–18,24,25], while other authors have used a 2′5′ADP Sepharose 4B affinity and anion exchange Q-Sepharose-4B columns [18–21]. It is interesting to mention that in all cases, individual bands of all mutant products were obtained with a purity of at least 96% when analyzed by SDS-PAGE [12,14,16–21,24,25]. Once the appropriate standardized protocol is implemented to obtain a large amount of the pure G6PD protein of each mutant strain, it is possible to execute functional and structural trials to correlate their residual activity with the corresponding clinical phenotype.

### 1.3. Functional Characterization of G6PD Variants

The World Health Organization working group classified G6PD variants into five classes based on the severity of the G6PD deficiency that accompanies the level of residual activity and hematological parameter of the patients. The Class I variants have the most severe manifestations with less than 5% of residual activity, while Class V are the mildest form [19,28,29]. Measurements of enzyme activity in red cells extracts did not give a reasonable indicator of the altered Michaelis constants of G6PD protein due to either a decreased level of enzyme with normal  $k_{cat}$ , or a normal level of enzyme with a decreased  $k_{cat}$ . Nevertheless, it is valuable to generate purified enzymes of quality to compare the kinetic properties of mutated enzymes vs. WT to understand the effect of the molecular alterations in the enzyme function [17].

#### G6PD Enzyme Kinetic Characterization

According to data obtained from the purified recombinant WT G6PD enzyme and reported by Wang et al. [25], the kinetics of G6PD obeyed a rapid-equilibrium random-order mechanism where any of the two substrates can bind independently to the enzyme before the catalytic event, which corresponded to the slowest reaction step. The G6PD kinetic parameters were determined using two methods. In the first method, the initial-rate equation for the two-substrate G6PD reaction was determined fluorimetrically in the Dalziel nomenclature [30]. In this method, a series of initial rate measurements was made with a constant initial concentration of Substrate 2 ( $S_2$ ) (not necessarily large) and different concentration of Substrate 1 ( $S_1$ ). In the second method, the kinetic parameters were determined spectroscopically by monitoring the reduction of NADP<sup>+</sup> at 340 nm [19–21]. The parameters were obtained by fitting initial velocity data by non-linear regression calculations. Initial velocity data were obtained by varying one substrate concentration with the second substrate fixed at saturating concentration.

Thus far, 20 G6PD variants have been purified and characterized functionally and structurally (Table 1). Table 3 summarizes the steady-state kinetic parameters of human G6PD variants of partially purified and recombinant enzyme. It can be observed that the  $k_{cat}$  values belonging to Class I G6PD mutants such as Zacatecas, Durham, Nashville, Volendam, Union and Andalus, dramatically decreased in their catalytic efficiency by around 75% with respect to WT. Furthermore, the Class II G6PD Santa-Maria showed a loss of catalysis of around 70%, while the other Class II mutants such as Valladolid, A+, Vanua-Lava and Viangchan only decreased 40%, respectively, when compared with WT G6PD. All these Class II variants were not associated with chronic hemolytic anemia or with acute hemolytic anemia [17,19]. In the case of Class I G6PD Nashville, Volendam and Zacatecas mutants, the  $K_m$  values were higher for the two physiological substrates with an affinity for physiological substrates of 3- and 4-fold lower compared to the WT G6PD enzyme. The degrees of enzymatic dysfunction detected in the mutants were in accordance with the severity of the clinical manifestations. Considering the reported clinical severity, it was especially striking that the Class I variants G6PD Plymouth, Wisconsin and Yucatan showed almost identical kinetic parameters to those of the WT enzyme [17–19].

However, there is a collection of variants for which a decrease in  $K_m$  values for both physiological substrates was observed; this group included the G6PD Union (Class I), Durham (Class I), Andalus (Class II), Valladolid Class II), Santa Maria (Class II), Vanua-Lava (Class II), Coimbra (Class II), and

Mexico City (Class III) variants. Although this change seemed favorable, these variant enzymes had a diminished catalytic efficiency at saturation levels of physiological substrates. It has been suggested that a better affinity for both physiological substrates is a compensatory mechanism due to a decrease in catalytic efficiency [21].

**Table 3.** Summary of catalytic properties of human recombinant G6PDs proteins.

G6PD	Class	$k_{cat}$ ( $s^{-1}$ )	$K_m$ G6P ( $\mu M$ )	$K_m$ NADP <sup>+</sup> ( $\mu M$ )	$k_{cat}/K_m$ G6P ( $s^{-1} M^{-1}$ )	$k_{cat}/K_m$ NADP <sup>+</sup> ( $s^{-1} M^{-1}$ )	References
WT <sup>1,2</sup>		233	38.5	6.2	$6.0 \times 10^6$	$37.8 \times 10^6$	[19]
Taipei <sup>1,2</sup>	I	n.d.	54.2	7.1	n.d.	n.d.	[14]
Volendam <sup>3,4</sup>	I	n.d.	328	51	n.d.	n.d.	[15]
Volendam <sup>1,2</sup>	I	n.d.	211	30	n.d.	n.d.	[15]
Andalus <sup>1,4</sup>	I	39.9	9.71	2.38	$4.11 \times 10^6$	$16.8 \times 10^6$	[16]
Wisconsin <sup>1,4</sup>	I	232	67.1	9.31	$3.52 \times 10^6$	$25.8 \times 10^6$	[17]
Nashville <sup>1,4</sup>	I	192	190	16.5	$1.02 \times 10^6$	$13.9 \times 10^6$	[17]
Plymouth <sup>1,4</sup>	I	207	50.7	6.46	$4.09 \times 10^6$	$32.1 \times 10^6$	[18]
Yucatan <sup>1,2</sup>	I	138	39.9	6.4	$3.5 \times 10^6$	$21.7 \times 10^6$	[19]
Nashville <sup>1,2</sup>	I	119	90.6	31.2	$1.3 \times 10^6$	$3.8 \times 10^6$	[19]
Durham <sup>1,2</sup>	I	71	24.77	6.96	$2.85 \times 10^6$	$10.2 \times 10^6$	[20]
Zacatecas <sup>1,2</sup>	I	58	111	24	$0.52 \times 10^6$	$2.41 \times 10^6$	[21]
Mahidol <sup>1,2</sup>	II	n.d.	48.5	8.2	n.d.	n.d.	[14]
Coimbra <sup>1,2</sup>	II	n.d.	15	6.2	n.d.	n.d.	[14]
Union <sup>1,4</sup>	II	28.6	9.53	2.76	$3.01 \times 10^6$	$10.5 \times 10^6$	[16]
Mahidol <sup>1,4</sup>	II	249	44.4	4.80	$5.60 \times 10^6$	$52.1 \times 10^6$	[18]
Valladolid <sup>1,2</sup>	II	96	21.5	3.6	$4.4 \times 10^6$	$26.2 \times 10^6$	[19]
Mexico-City <sup>1,2</sup>	III	182	24.9	9.1	$7.3 \times 10^6$	$19.1 \times 10^6$	[19]
Santa-Maria <sup>1,2</sup>	II	71	15.35	9.06	$4.62 \times 10^6$	$7.83 \times 10^6$	[20]
<sup>a,b</sup> A+	III	114	56.44	12.97	$2.02 \times 10^6$	$8.78 \times 10^6$	[20]
Vanua-Lava <sup>1,2</sup>	II	142	34	18	$4.17 \times 10^6$	$7.88 \times 10^6$	[21]
Viangchan <sup>1,2</sup>	II	145	42	17	$3.45 \times 10^6$	$8.52 \times 10^6$	[21]
Viangchan <sup>1,2</sup>	II	116	56.3	34.1	$2.0 \times 10^6$	$3.4 \times 10^6$	[22]
Mahidol <sup>1,2</sup>	II	224	46.9	5.9	$4.8 \times 10^6$	$38.1 \times 10^6$	[22]
Viangchan + Mahidol <sup>1,2</sup>	II/III	104	54.3	55.9	$1.9 \times 10^6$	$1.9 \times 10^6$	[22]
A <sup>-</sup>	III		74	15	n.d.	n.d.	[23]

Roman numerals indicate the class of each variant. <sup>1</sup> Recombinant. <sup>2</sup> Measured at 340 nm spectrophotometrically. <sup>3</sup> Erythrocyte. <sup>4</sup> Fluorescence spectrophotometer. n.d. = not determined.

It is noteworthy that variants with mutations located in different regions of the protein 3D structure (Figure 2) showed lower catalytic activities ( $k_{cat}$ ) than WT G6PD (Table 3). These data suggest that catalytic efficiency is affected by these mutations despite their location in the tertiary structure (Figure 2).

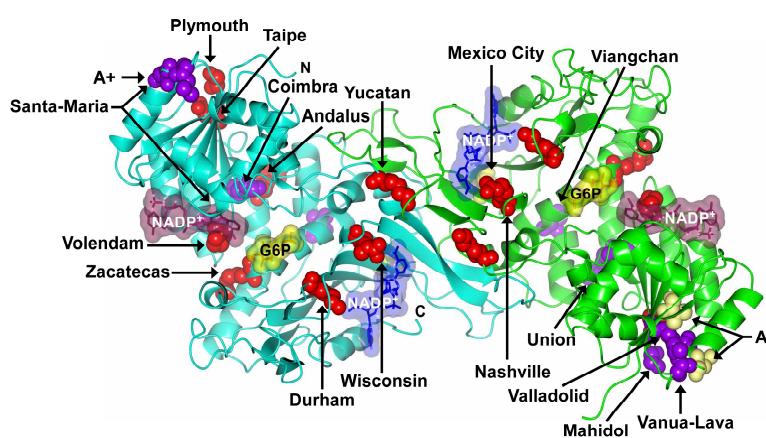


**Figure 2.** Location of single nucleotide substitutions (missense variants) in G6PD structure showing Class I (red spheres), Class II (purple spheres), and Class III (yellow spheres) mutations. Note that the illustration only shows Zacatecas, Durham, Yucatan, Viangchan, Coimbra, Volendam, Mexico City, Vanua-Lava and Taipei mutants on equivalent positions of the G6PD dimer.

#### 1.4. Structural Characterization of Glucose-6-Phosphate Dehydrogenase Variants

##### 1.4.1. Analysis of the Stability of the G6PD Enzymes

According to Huang et al. [18], reduced activity of G6PD mutated enzymes could be explained by an impairment of accurate folding of the protein, altered dimer formation, or by a quantitative diminution of the expressed protein as a consequence of pre-mRNA splicing disruption [18]. Several studies have focused on the examination of the molecular mechanisms regarding the reduction of G6PD activity observed in patients at the protein level [17,18,23,29,31]. However, the main question is whether the poor enzyme activity of the G6PD mutants in a relatively long-lived non-nucleate cell is due to instability of the active form or if they are kinetically defective [16]. In this regard, Cunningham et al. [32] demonstrated that the clinical phenotypes of G6PD variants were largely determined by a trade-off between protein stability and catalytic activity by using a multidimensional analysis of biochemical data.

##### 1.4.2. Thermostability

Diverse studies have suggested that the structural instability of the G6PD protein could be the most frequent deleterious effect caused by mutations and could explain the clinical manifestations of G6PD deficiency. Measuring thermostability is a useful strategy to assess the impact of the different mutations on protein structure, stability and activity of the G6PD [9,18,33,34]. In fact, thermal inactivation of WT G6PD and pathological mutants has been analyzed with different concentrations of NADP<sup>+</sup> (from 0–1 mM). In the absence of added NADP<sup>+</sup>, the  $T_{50}$  value experimentally has been determined (Table 4). The range of  $T_{50}$  values, obtained without NADP<sup>+</sup>, for G6PD Class I variants Nashville, Yucatan, Durham, Zacatecas, Andalus, Fukaya, Campinas and Class II G6PD Viangchan, Mahidol and Mahidol + Viangchan, showed a striking reduction of 6–14 °C in its thermostability in vitro compared to WT G6PD (Table 4) [16–19,21,22,27]. The reduction in the thermostability of G6PD variants with mutations in exons 10 and 11 is congruent with previously reported clinical manifestations and symptoms associated with the variants such as CNSHA. The observed thermal inactivation point indicates that these enzymes are more sensitive to temperature dependent denaturation, suggesting that mutations in these G6PD Class I variants result in a more unstable and relaxed active site. Nonetheless, the Class I mutants Wisconsin and Plymouth are more heat resistant than other Class I mutants (Table 4), even though they have been associated with CNSHA. In the same sense, G6PD Class II and III variants Santa-Maria, Valladolid, Mahidol, Vanua-Lava, A+ and Mexico City were slightly less thermostable compared to WT, suggesting that the decreased activity was due to causes other than the instability of the active site [20].

**Table 4.** Summary of thermal inactivation and melting temperature assays for the WT and G6PD variants.

G6PD	Class	$T_{50}$ (°C)		$T_m$ (°C)	Reference
		Without NADP <sup>+</sup>	With NADP <sup>+</sup>		
WT		44	60 <sup>1</sup>	n.d	[16]
WT		47	62 <sup>1</sup>	n.d	[18]
WT		46	58 <sup>1</sup>	55.5	[27]
WT		47	n.d	51.5	[26]
WT		52.1	62 <sup>2</sup>	55	[19]
WT		47	54 <sup>2</sup>	54.8	[20]
WT		48	58 <sup>2</sup>	59	[21]
WT		47	57 <sup>1</sup>	54.8	[22]
Andalus	I	40	54 <sup>1</sup>	n.d	[16]
Plymouth	I	42	57 <sup>1</sup>	n.d	[18]
Wisconsin	I	46	59 <sup>1</sup>	55.5	[27]
Nashville	I	39	52 <sup>1</sup>	50	[27]
Fukaya	I	39	51 <sup>1</sup>	48.5	[27]

Table 4. Cont.

G6PD	Class	$T_{50}$ (°C)		$T_m$ (°C)	Reference
		Without NADP <sup>+</sup>	With NADP <sup>+</sup>		
Campinas	I	34	39 <sup>1</sup>	45.5	[27]
Yucatan	I	45.8	51 <sup>2</sup>	53	[19]
Nashville	I	45.3	48 <sup>2</sup>	50	[19]
Durham	I	40.3	42 <sup>2</sup>	49.9	[20]
Zacatecas	I	41	51 <sup>2</sup>	48	[21]
Union	II	41	54	n.d.	[16]
Mahidol	II	42	57 <sup>1</sup>	n.d.	[18]
Valladolid	II	49	59 <sup>2</sup>	53	[19]
Santa-Maria	II	45.5	52 <sup>2</sup>	54.8	[20]
A+	III	45.6	54 <sup>2</sup>	55.8	[20]
Vanua-Lava	II	47	57 <sup>2</sup>	45	[21]
Viangchan	II	41	51 <sup>2</sup>	53.4	[21]
Viangchan	II	37.5	51 <sup>1</sup>	42.7	[22]
Mahidol	II	42	52 <sup>1</sup>	45.5	[22]
Viangchan + Mahidol	II/III	33.5	49 <sup>1</sup>	37.7	[22]
Mexico City	III	48.2	58 <sup>2</sup>	53	[19]

Thermal inactivation ( $T_{50}$ ) assays in the presence of <sup>1</sup> 1000 and <sup>2</sup> 500  $\mu$ M of NADP<sup>+</sup>. Thermal unfolding ( $T_m$ ) of WT G6PD and variants has been monitored by recording the change in CD signal at 222 nm at different temperatures ranging from 20 to 90 °C. n.d = not determined.

#### 1.4.3. Structural and Biochemical Characterization

Structural and biochemical studies concerning the G6PD enzyme and its variants have indicated that structural NADP<sup>+</sup> is essential for both stability and enzymatic activity. Using thermostability assays, it has been demonstrated that high concentrations of NADP<sup>+</sup> increase the stability of some G6PD enzyme variants. For example,  $T_{50}$  values for enzymes of Class I, II, and III variants such as G6PD Yucatan [19], Mahidol [18], Andalus [16], Plymouth [18], Zacatecas [21], Viangchan [21], Valladolid [19], Vanua-Lava [21], Mexico City [19], A<sup>-</sup> [19], and Union [16] were 10 °C higher when NADP<sup>+</sup> concentrations were increased (Table 4) compared to the temperature obtained without NADP<sup>+</sup>. It is noteworthy that these mutations were not located near the active site or the structural NADP<sup>+</sup> binding site in the native G6PD enzyme (Figure 3A). Nonetheless, very interesting exceptions were seen for Class I G6PD mutants Nashville [17,19], Campinas [27] and Durham [21] where the protective effect was not observed when NADP<sup>+</sup> was increased (Table 4). These findings could be explained because mutations located near the dimer interface and structural NADP<sup>+</sup> binding site could conceivably cause impairment in the dimer conformation or in the binding capacity of structural NADP<sup>+</sup> (Figure 3B).

#### 1.4.4. Stability in the Presence or Absence of Urea, Protease Digestion and NADP<sup>+</sup>

The assumption that the structural instability of G6PD is the most frequent deleterious effect has allowed the evaluation of the enzymatic activity in vitro resembling physiological and stringent conditions with denaturing agents such as urea and protease digestion in the presence or absence of NADP<sup>+</sup>. Time-courses of loss of activity of WT G6PD and the mutants G6PD Plymouth, Mahidol, Durham, A+ and Santa Maria [9,18,20] without NADP<sup>+</sup> have been performed. Huang et al. [18] observed that when the G6PD Plymouth and Mahidol mutants were incubated at a physiological temperature (37 °C) and pH (7.2), an important reduction in the stability of both proteins was observed after 24 h of storage as they were only capable of retaining 27% and 4% of enzymatic activity, respectively. Moreover, Gomez-Manzo et al. [20] performed a similar stability assay on three different mutants. They found that G6PD Durham, A+ and Santa Maria variants diminished their activity around 73%, 40% and 20%, respectively, when compared with the WT G6PD enzyme after 90 min of storage; however, upon adding a physiological concentration of NADP<sup>+</sup> (10  $\mu$ M), a protective effect of NADP<sup>+</sup> was observed for all mutants. Other studies carried out by Wang et al. [17] determined the

stability of WT G6PD and two Class I variants (Nashville and Wisconsin) with different concentrations of urea in the presence or absence of  $\text{NADP}^+$  and showed that without this cofactor, the three enzymes were very susceptible to urea, losing close to 80% of their activity. However, for all three enzymes,  $\text{NADP}^+$  (10  $\mu\text{M}$ ) offered protection against urea denaturation, but this protector effect was partial in the case of Arg393His [17]. Following the analysis of structural stability in other recombinant human mutants, Gomez-Manzo et al. [21] performed inactivation assays with guanidine hydrochloride (Gdn-HCl) for G6PD Zacatecas, Vanua-Lava and Viangchan mutants. Their results showed a faster loss of activity for Class I G6PD Zacatecas and Class II G6PD Viangchan variants; furthermore, both mutants were highly susceptible to Gdn-HCl treatment, showing a total loss of enzyme activity with 0.25 M Gdn-HCl. Together, these results suggest that Class I G6PD variants (that include Plymouth, Durham, Nashville, Zacatecas and Class II G6PD Viangchan), had a lower conformational stability and a relaxed active site with respect to the WT G6PD enzyme [18,20]. The lack of activity triggered by the presence of denaturing agents agrees with the protective effect of  $\text{NADP}^+$ . The mutants where  $\text{NADP}^+$  increases did not protect were the same mutants that lost their activity more quickly.

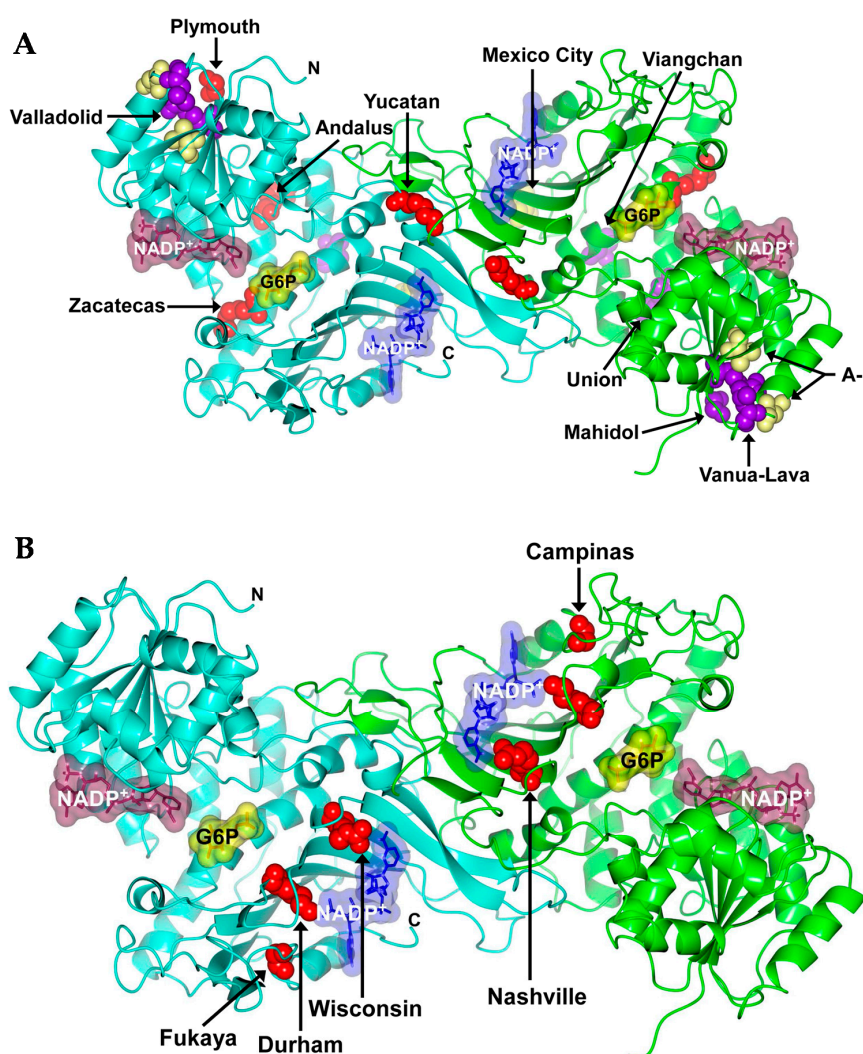


**Figure 3.** Position of mutations in G6PD affecting its thermostability. Location of Class I (red spheres), Class II (purple spheres), and Class III (yellow spheres) mutations in G6PD structure that showed (A) a protective; and (B) not protective effect when  $\text{NADP}^+$  was increased. Note that although most of the mutants are located on equivalent positions of G6PD dimer, Fukaya, Campinas, Wisconsin, Nashville, Plymouth, Mahidol, Union and Andalus mutants are shown in only one of the monomers.

Different studies have proposed that defects in protein folding not only reduces protein stability, but also accelerate its degradation. To explore this idea, Wang et al. [17] performed protein digestion of WT G6PD and Class I G6PD Nashville, Wisconsin, Fukaya and Campinas using trypsin and chymotrypsin with different NADP<sup>+</sup> concentrations. The results showed that the Nashville variant was more susceptible to proteolysis with both proteases; Fukaya and Campinas mutants [27] were unstable at room temperature compared with WT in presence of chymotrypsin; whereas all mutants incubated with NADP<sup>+</sup> became more resistant to chymotrypsin degradation. Boonyuen et al. [22] studied the susceptibility to trypsin digestion for Class II G6PD Viangchan and Class II G6PD Mahidol variants with NADP<sup>+</sup>; their results showed that both variants showed the same susceptibility to trypsin digestion vs. the native enzyme. Of note was that the presence of NADP<sup>+</sup> improved the stability against proteolysis of the afore-mentioned variants. Additionally, unfolding and refolding experiments of WT and the mutant G6PD enzymes (Class I G6PD Nashville, Wisconsin, Fukaya and Campinas) were carried out [27]. The reported results showed that the four mutants exhibited impairments in the *in vitro* refolding process, suggesting that such a disturbance could also be present *in vivo*. This decreased refolding capacity of the G6PD variants correlated with their lower binding ability for “structural” NADP<sup>+</sup>, suggesting that under these experimental conditions, NADP<sup>+</sup> is essential in the refolding process [27].

#### 1.4.5. Spectroscopic Characterization

Spectroscopic characterization by circular dichroism (CD) is used extensively to study the structural changes of proteins. Measurements carried out for G6PD variants have shown that Nashville, Wisconsin, Plymouth, Mahidol, Viangchan, Yucatan, Valladolid, Mexico City, Durham, Santa Maria, A+, Zacatecas and Vanua-Lava did not show significant changes in their secondary structure, suggesting that the phenotype produced by these variants was probably due to the loss of stability of each mutant, or the loss of catalytically competent conformation of the active site [19–22,27]. Thermal denaturation characterization of the G6PD enzymes is another approach that has been used to evaluate alterations in the protein structure [9,16,18,34]. Using this method,  $\Delta T_m$  has been observed around to 5–12 °C for the G6PD Nashville, Fukaya, Campinas, Durham, Zacatecas, Viangchan, Vanua-Lava and Mahidol variants; while variants such as G6PD Yucatan, Valladolid, Mexico City, and A+ showed a  $\Delta T_m$  about 2 °C lower with respect to the WT G6PD enzyme (Table 4). These differences in  $\Delta T_m$  indicate that some mutations have a strong effect on structure stability, which could be responsible for clinical manifestations [21].

#### 1.4.6. Analysis of Conformational Changes

Intrinsic fluorescence and 8-Anilino-naphthalene-1-sulphonate (ANS) assays have been performed to evaluate the global structure of proteins. Specifically, the presence of seven tryptophan residues/monomer in human G6PD can be used to evaluate its tertiary structure by intrinsic fluorescence [6], whereas maximum fluorescence emission has been successfully used to monitor changes in the microenvironment of tryptophan residues. The intrinsic fluorescent intensity for the Class I G6PD Zacatecas, Durham and Class II G6PD Santa-Maria, Viangchan and A+ variants presented 1.4 to 2-fold increases; while for G6PD Vanua-Lava changes with respect to WT G6PD were not detected. Gomez-Manzo et al. [21] suggested that increased intensity of intrinsic fluorescence for Class I G6PD Zacatecas (Arg257Leu) could be due to microenvironmental modifications by Trp462 residues which contribute to the re-location of the tryptophan into a more hydrophilic environment in 3D structure. In the WT enzyme, the Arg257 forms a weak cation– $\pi$  interaction with W462, which is lost in the R257L mutant [21]. A different pattern of intrinsic fluorescence intensity has also been detected for the Class I G6PD Durham (Lys238Arg) variant, probably because the mutation (Lys238Arg) is situated near of structural NADP<sup>+</sup> binding site. The replacement of Lysine by Arginine residue implies an increase of 25 Å<sup>2</sup> in the surface area that probably induces steric hindrance, causing the side-chain of arginine

to rotate away from structural  $\text{NADP}^+$ , and consequently lead to a less stable  $\text{NADP}^+$ -bound form (Figure 4) [20].

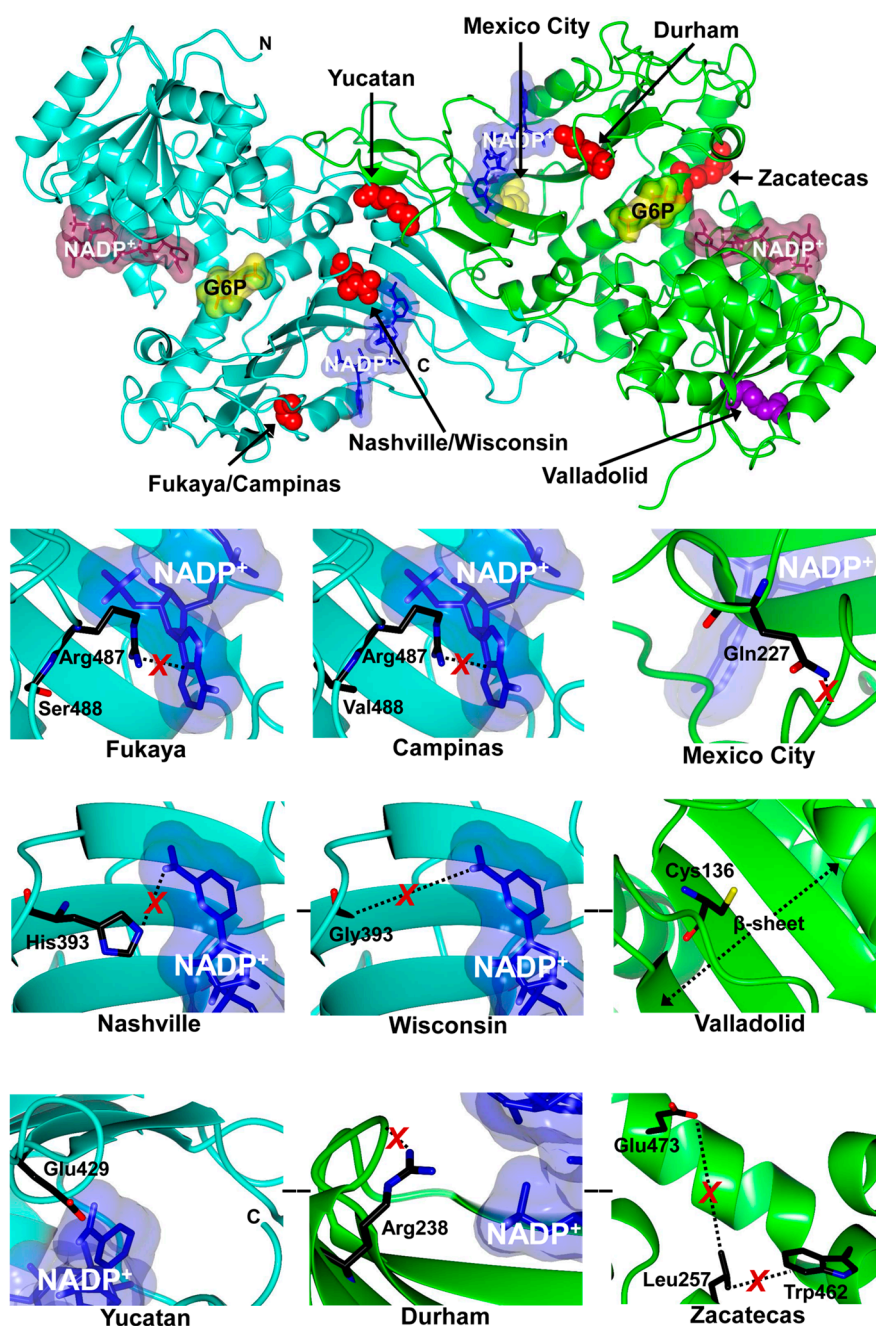


**Figure 4.** Location of single nucleotide substitutions in G6PD dimer. Insets, close-up of Gly488 mutated either by Ser (Class I, G6PD Fukaya) or Val (Class I, G6PD Campinas). Arg393 replaced by His (G6PD Nashville) or Gly (G6PD Wisconsin). Arg227 replaced by Gln in G6PD Mexico City variant. Arg136 replaced by Cys in G6PD Valladolid variant. Lys429 replaced by Glu in G6PD Yucatan variant. Arg257 replaced by Leu in G6PD Zacatecas variant and Lys238 replaced by Arg in G6PD Durham variant. Mutants of G6PD dimer are indicated by colored spheres: Class I in red, Class II in purple, and Class III in yellow. Mutants in the insets are shown as black cylinders. “X” represents the loss of interaction or clash that is generated in each mutation and affects the native enzyme. Note that all mutants are shown in only one of the monomers of G6PD enzyme.

Furthermore, 8-Anilino-naphthalene-1-sulphonate (ANS) assays are used to monitor the conformational changes of proteins. An increased fluorescence level suggests full exposure of hydrophobic sites to the solvent, therefore a higher ANS fluorescence means more exposed hydrophobic regions [17,19,35]. In ANS assays, G6PD showed that fluorescence emission increased 1.8, 2, 2.6, 3 and 7.5-fold for the G6PD Valladolid (Class II), Nashville (Class I), Durham (Class I), Mexico City (Class II) and Zacatecas (Class I) variants, respectively, when compared with WT G6PD (Table 5) [19–21]; while G6PD Wisconsin (Class I), Santa-Maria (Class II), Vanua-Lava (Class II), Viangchan (Class II) and A+ (Class II) variants showed only a slight increase in the ANS spectra compared to WT G6PD (Table 5) [17,19–21,35]. Nonetheless, the Class I G6PD Yucatan was the only variant that showed a decrease in fluorescence intensity relative to WT G6PD [19]. The increased changes in fluorescence intensity observed for G6PD Valladolid, Nashville, Durham, Mexico-city, and Zacatecas variants suggest that these mutants have altered structure with more hydrophobic surfaces accessible to the dye probe. These changes could accelerate the aggregation of the G6PD mutants and favor the degradation of G6PD variants in vivo and could conceivably trigger the clinical manifestations of the disease.

**Table 5.** Analysis of conformational changes by 8-Anilino-naphthalene-1-sulphonate (ANS) assay for the WT and G6PD variants.

G6PD	Codon and Amino Acid Substitution	Class	Ratio of Fluorescence (F/F <sub>0</sub> )	Reference
Wisconsin <sup>2</sup>	Arg393Gly	I	1	[17]
Nashville <sup>2</sup>	Arg393His	I	2.2	[17]
Yucatan <sup>1</sup>	Lys429Glu	I	1	[19]
Nashville <sup>1</sup>	Arg393His	I	2.6	[19]
Durham <sup>1</sup>	Lys238Arg	I	2.6	[20]
Zacatecas <sup>1</sup>	Arg257Leu	I	7.9	[21]
Valladolid <sup>1</sup>	Arg136Cys	II	1.8	[19]
Santa Maria <sup>1</sup>	Asn126Asp	II	1	[20]
A <sup>1</sup>	Asp181Val	III	1.3	[36]
A+ <sup>1</sup>	Asn126Asp	III	1	[20]
Vanua-Lava <sup>1</sup>	Lys128Pro	II	1.2	[21]
Viangchan <sup>1</sup>	Val291Met	II	1.5	[21]
Mexico City <sup>1</sup>	Arg227Gln	III	4	[19]
A <sup>-1</sup>	Ans126Asp Val68Met	III	1.8	[36]

The ratio of the fluorescence of WT G6PD (F<sub>0</sub>) and mutants (F) was determined in the <sup>1</sup> absence or <sup>2</sup> presence of 2 M urea incubated at 2 h.

Finally, an analysis of oligomeric protein structure was performed by gel filtration chromatography to explore changes in the quaternary structure of G6PD variants. The results showed that both WT and variants G6PD Zacatecas, Vanua-Lava, and Viangchan elute as native dimers, indicating that alterations in the specific activity of these mutants was not due to the dissociation of the proteins either in the presence, or absence of denaturing agents [21]. In this context, Wang et al. [9] determined a gel-elution profile of native and stripped G6PD (intact holoenzyme). Their results showed that at a lower concentration, G6PD protein may acquire both dimer and tetramer structures (seen as two peaks); however, when the concentration of both proteins was increased, these merged into a single peak corresponding closely to the value for a trimer. Interestingly, native G6PD saturated with structural NADP<sup>+</sup> gave rise to a rapidly adjusting dimer–tetramer equilibrium. In contrast, when the structural NADP<sup>+</sup> was stripped from the G6PD, the formation of tetramer was suppressed [9].

## 2. Computer Modelling

Based on the human G6PD three-dimensional structure, previous studies have reported that amino acid sequence mutations can explain altered biochemical function of G6PD. In this context, Wang et al. [9] showed that Glycine 488 was important in positioning Arginine 487 that interacted

directly with the structural NADP<sup>+</sup>. Additionally, whether Glycine 488 was mutated either by Serine (Class I, G6PD Fukaya) [27] or Valine (Class I, G6PD Campinas) (Figure 4) [27], they observed via biochemical studies that structural NADP<sup>+</sup>-dependent binding increased around 7- and 13-fold for the G6PD Fukaya and G6PD Campinas compared to WT G6PD. Such results clearly showed that these mutations affected the binding affinity for structural NADP<sup>+</sup>.

A similar analysis was performed for two Class I mutants (Arginine 393 was replaced by Histidine (G6PD Nashville) and Glycine (G6PD Wisconsin) where the *in silico* analysis showed that Arginine 393 was found in the dimer interface and interacted with the structural NADP<sup>+</sup> [17]. The replacement of Arg 393 by Gly caused the loss of interaction with the structural NADP<sup>+</sup> (Figure 4). These authors concluded that these mutations affected the interaction between the structural NADP<sup>+</sup> and the dimer interface, causing instability of the mutant enzymes [17].

Furthermore, Gómez-Manzo et al. [20] observed using this same approach that in the G6PD Mexico City variant (when Arg227 was substituted with a glutamine residue), a steric hindrance should be generated, affecting the conformation of the protein and causing the disease phenotype [19] (Figure 4), although the point mutation was distant from the active site or the dimer interface. With respect to the Yucatan G6PD variant (Lys429Glu), Gómez-Manzo et al. [19] reported that between the C-terminal and the Glutamic acid 429 amino acid there was a negative environment, which could promote a repulsion phenomenon due to the negative (Figure 4). This phenomenon could increase instability affecting the interactions with structural NADP<sup>+</sup> and consequently the global stability of G6PD [19].

In this sense, Gómez-Manzo et al. [20] reported that the clinical manifestations of the G6PD Durham (Lys238Arg) variant were probably due to the mutation located near the structural NADP<sup>+</sup> binding site where the replacement of Lysine by Arginine residue implied an increase in the surface area of the side chain of 1.12-fold (200 to 225 Å<sup>2</sup>) [37]. Furthermore, in Class I G6PD Zacatecas (Arg257Leu), Arginine was replaced by Leucine and induced the loss of a salt bridge between Arg257 and Glu473 (Figure 4), which are highly conserved amino acids in different organisms. In addition, this mutation provoked the loss of the cation- $\pi$  interaction between Arg257 and Trp462, suggesting that the three-dimensional structure was to some extent open, and presented a loss of the secondary structure exposing hydrophobic regions on the mutant enzyme [21].

### 3. Conclusions

G6PD deficiency is the most common enzymopathy, leading to alterations in the first step of the pentose phosphate pathway which interferes with the protection of the erythrocyte against oxidative stress, and causes a wide range of clinical symptoms of which hemolysis is one of the most severe. Recently, an extensive review was published, recognizing 217 mutations in the G6PD gene that are responsible for the severity of the clinical symptoms. To understand the molecular basis of the deficiency, several groups have characterized the functional and structural effects of some mutations. In this review, we described and compared the biochemical profile of 20 different G6PD variants in detail and its probable relationship with the impairment of enzyme function. The methods to achieve the most representative behavior of the variant and the best kinetic parameters to compare between variants were addressed, as well as an analysis of protein stability by different assays and tools. The impairment in the enzymatic activity of each variant appeared to be related to alterations in the ligand binding site, or structural stability leading to a shorter half-life or misfolding of the protein. This characterization was related with the clinical outcome, allowing a better understanding of the G6PD mutants and a concomitant management for the patients.

**Acknowledgments:** Saúl Gómez-Manzo is supported by CONACyT grants 154570 and INP 055/2015; America Vanoye-Carlo is supported by CONACyT grants 157863 and INP 089/2012; Jaime Marcial-Quino is supported by CONACYT grant 259201 and Cátedras CONACYT (2184) project number 2057. Edgar Sierra-Palacios is supported by the Universidad Autónoma de la Ciudad de México with the agreement UACM-SECITI-DF-060-2013, project number PI2013-59. The technical assistance of Maria Jose Gomez-Gonzalez, Ximena Gomez-Gonzalez, and Camila Marcial are greatly appreciated. Finally, thanks to Javier Gallegos Infante (Instituto de Fisiología Celular, UNAM) for assistance with bibliographic materials.

**Author Contributions:** Saúl Gómez-Manzo, Jaime Marcial-Quino and America Vanoye-Carlo conceived and designed the paper. Hugo Serrano-Posada, Abigail González-Valdez and Beatriz Hernández-Ochoa performed the figures and tables. Daniel Ortega-Cuellar, Edgar Sierra-Palacios, Adriana Castillo-Villanueva and Horacio Reyes-Vivas analyzed the information. All authors wrote the manuscript.

**Conflicts of Interest:** The authors declare no conflict of interest.

## References

1. Vulliamy, T.J.; D'Urso, M.; Battistuzzi, G.; Estrada, M.; Foulkes, N.S.; Martini, G.; Calabro, V.; Poggi, V.; Giordano, R.; Town, M.; et al. Diverse point mutations in the human glucose-6-phosphate dehydrogenase gene cause enzyme deficiency and mild or severe hemolytic anemia. *Proc. Natl. Acad. Sci. USA* **1998**, *85*, 5171–5175. [[CrossRef](#)]
2. Gómez-Manzo, S.; Marcial-Quino, J.; Vanoye-Carlo, A.; Serrano-Posada, H.; Ortega-Cuellar, D.; González-Valdez, A.; Castillo-Rodríguez, R.A.; Hernández-Ochoa, B.; Sierra-Palacios, E.; Rodríguez-Bustamante, E.; et al. Glucose-6-Phosphate Dehydrogenase: Update and Analysis of New Mutations around the World. *Int. J. Mol. Sci.* **2016**, *17*, 2069. [[CrossRef](#)] [[PubMed](#)]
3. Cappellini, M.D.; Fiorelli, G. Glucose-6-phosphate dehydrogenase deficiency. *Lancet* **2008**, *9606*, 64–74. [[CrossRef](#)]
4. Persico, M.G.; Viglietto, G.; Martini, G.; Toniolo, D.; Paonessa, G.; Moscatelli, C.; Dono, R.; Vulliamy, T.; Luzzatto, L.; D'Urso, M. Isolation of human glucose-6-phosphate dehydrogenase (G6PD) cDNA clones: Primary structure of the protein and unusual 50 non-coding region. *Nucleic Acids Res.* **1986**, *14*, 2511–2522. [[CrossRef](#)] [[PubMed](#)]
5. Rattazzi, M.C. Glucose 6-phosphate dehydrogenase from human erythrocytes: Molecular weight determination by gel filtration. *Biochem. Biophys. Res. Commun.* **1968**, *31*, 16–24. [[CrossRef](#)]
6. Au, S.W.N.; Gover, S.; Lam, V.; Adams, M. Human glucose-6-phosphate dehydrogenase: The crystal structure reveals a structural NADP<sup>+</sup> molecule and provides insights into enzyme deficiency. *Structure* **2000**, *8*, 293–303. [[CrossRef](#)]
7. Au, S.W.; Naylor, C.E.; Gover, S.; Vandeputte-Rutten, L.; Scopes, D.A.; Mason, P.J.; Luzzatto, L.; Lam, V.M.; Adams, M.J. Solution of the structure of tetrameric human glucose 6-phosphate dehydrogenase by molecular replacement. *Acta Crystallogr. D Biol. Crystallogr.* **1999**, *55*, 826–834. [[CrossRef](#)] [[PubMed](#)]
8. Kotaka, M.; Gover, S.; Vandeputte-Rutten, L.; Au, S.W.N.; Lam, V.M.S.; Adams, M.J. Structural studies of glucose-6-phosphate and NADP<sup>+</sup> binding to human glucose-6-phosphate dehydrogenase. *Acta Crystallogr. D Biol. Crystallogr.* **2005**, *61*, 495–504. [[CrossRef](#)] [[PubMed](#)]
9. Wang, X.T.; Chan, T.F.; Lam, V.; Engel, P. What is the role of the second “structural” NADP<sup>+</sup>-binding site in human glucose-6-phosphate dehydrogenase? *Protein Sci.* **2008**, *17*, 1403–1411. [[CrossRef](#)] [[PubMed](#)]
10. Fiorelli, G.; di Montemuros, F.M.; Cappellini, M. Chronic nonspherocytic hemolytic disorders associated with glucose-6-phosphate dehydrogenase variants. *Baillière's Clin. Haematol.* **2000**, *13*, 39–55.
11. McNicholas, S.; Potterton, E.; Wilson, K.S.; Noble, M.E.M. Presenting your structures: The CCP4mg molecular-graphics software. *Acta Crystallogr. D Biol. Crystallogr.* **2011**, *67*, 386–394. [[CrossRef](#)] [[PubMed](#)]
12. Bautista, J.M.; Mason, P.J.; Luzzatto, L. Human glucose-6-phosphate dehydrogenase Lysine 205 is dispensable for substrate binding but essential for catalysis. *FEBS Lett.* **1995**, *366*, 61–64. [[CrossRef](#)]
13. Cheng, Y.S.; Tang, T.K.; Hwang, M.J. Amino acid conservation and clinical severity of human glucose-6-phosphate dehydrogenase mutations. *J. Biomed. Sci.* **1999**, *6*, 106–114. [[CrossRef](#)] [[PubMed](#)]
14. Tang, T.K.; Yeh, C.H.; Huang, C.S.; Huang, M.J. Expression and biochemical characterization of human glucose-6-phosphate dehydrogenase in *Escherichia coli*: A system to analyze normal and mutant enzymes. *Blood* **1994**, *83*, 1436–1441. [[PubMed](#)]
15. Roos, D.; Van Zwieten, Z.R.; Wijnen, J.T.; Gomez-Gallego, F.; De Boer, B.M.; Stevens, D.; Pronk-Admiraal, C.J.; de Rijk, T.; van Noorden, C.J.; Weening, R.S.; et al. Molecular basis and enzymatic properties of glucose 6-phosphate dehydrogenase volendam, leading to chronic nonspherocytic anemia, granulocyte dysfunction, and increased susceptibility to infections. *Blood* **1999**, *94*, 2955–2962. [[PubMed](#)]
16. Wang, X.T.; Lam, V.M.; Engel, P.C. Marked decrease in specific activity contributes to disease phenotype in two human glucose-6-phosphate dehydrogenase mutants, G6PDUnion and G6PDAndalus. *Hum. Mutat.* **2005**, *26*, 284–293. [[CrossRef](#)] [[PubMed](#)]

17. Wang, X.T.; Lam, V.M.S.; Engel, P.C. Functional properties of two mutants of human glucose 6-phosphate dehydrogenase, R393G and R393H, corresponding to the clinical variants G6PD Wisconsin and Nashville. *Biochim. Biophys. Acta* **2006**, *1762*, 767–774. [[CrossRef](#)] [[PubMed](#)]
18. Huang, Y.; Choi, M.Y.; Au, S.W.; Au, D.M.; Lam, V.M.S.; Engel, P.C. Purification and detailed study of two clinically different human glucose 6-phosphate dehydrogenase variants, G6PD (Plymouth) and G6PD (Mahidol): Evidence for defective protein folding as the basis of disease. *Mol. Genet. Metab.* **2008**, *93*, 44–53. [[CrossRef](#)] [[PubMed](#)]
19. Gómez-Manzo, S.; Terrón-Hernández, J.; De la Mora-De la Mora, I.; González-Valdez, A.; Marcial-Quino, J.; García-Torres, I.; Vanoye-Carlo, A.; López-Velázquez, G.; Hernández-Alcantara, G.; Oria-Hernández, J.; et al. The stability of G6PD is affected by mutations with different clinical phenotypes. *Int. J. Mol. Sci.* **2014**, *15*, 21179–21201. [[CrossRef](#)] [[PubMed](#)]
20. Gómez-Manzo, S.; Marcial-Quino, J.; Vanoye-Carlo, A.; Enríquez-Flores, S.; De la Mora-De la Mora, I.; González-Valdez, A.; García-Torres, A.; Martínez-Rosas, V.; Sierra-Palacios, E.; Lazcano-Pérez, F.; et al. Mutations of Glucose-6-Phosphate Dehydrogenase Durham, Santa-Maria and A+ Variants Are Associated with Loss Functional and Structural Stability of the Protein. *Int. J. Mol. Sci.* **2015**, *16*, 28657–28668. [[CrossRef](#)] [[PubMed](#)]
21. Gómez-Manzo, S.; Marcial-Quino, J.; Vanoye-Carlo, A.; Serrano-Posada, H.; González-Valdez, A.; Martínez-Rosas, V.; Hernández-Ochoa, B.; Sierra-Palacios, E.; Castillo-Rodríguez, R.A.; Cuevas-Cruz, M.; et al. Functional and biochemical characterization of three recombinant human Glucose-6-Phosphate Dehydrogenase mutants: Zacatecas, Vanua-Lava and Viangchan. *Int. J. Mol. Sci.* **2016**, *17*, E787. [[CrossRef](#)] [[PubMed](#)]
22. Boonyuen, U.; Chamchoy, K.; Swangsri, T.; Saralamba, T.; Day, N.P.J.; Imwong, M. Detailed functional analysis of two clinical glucose-6-phosphate dehydrogenase (G6PD) variants, G6PDViangchan and G6PDViangchan + Mahidol: Decreased stability and catalytic efficiency contribute to the clinical phenotype. *Mol. Genet. Metab.* **2016**, *2*, 84–91. [[CrossRef](#)] [[PubMed](#)]
23. Gomez-Gallego, F.; Garrido-Pertierra, A.; Mason, P.J.; Bautista, J.M. Unproductive folding of the human G6PD-deficient variant A. *FASEB J.* **1996**, *10*, 153–158. [[PubMed](#)]
24. Bautista, J.M.; Mason, P.J.; Luzzatto, L. Purification and properties of human glucose-6-phosphate dehydrogenase made in *E. coli*. *Biochim. Biophys. Acta* **1992**, *1119*, 74–80. [[CrossRef](#)]
25. Wang, X.T.; Au, S.W.N.; Lam, V.M.S.; Engel, P.C. Recombinant human glucose-6-phosphate dehydrogenase: Evidence for a rapid-equilibrium random-order mechanism. *Eur. J. Biochem.* **2002**, *269*, 3417–3424. [[CrossRef](#)] [[PubMed](#)]
26. Gómez-Manzo, S.; Terrón-Hernández, J.; de la Mora-de la Mora, I.; García Torres, I.; López-Velázquez, G.; Reyes-Vivas, H.; Oria-Hernández, J. Cloning, expression, purification and characterization of His-tagged human glucose-6-phosphate dehydrogenase: A simplified method for protein yield. *Protein J.* **2013**, *32*, 585–592. [[CrossRef](#)] [[PubMed](#)]
27. Wang, X.T.; Engel, P.C. Clinical mutants of human glucose-6-phosphate dehydrogenase: Impairment of NADP<sup>+</sup> binding affects both folding and stability. *Biochim. Biophys. Acta* **2009**, *1792*, 804–809. [[CrossRef](#)] [[PubMed](#)]
28. Vulliamy, T.; Luzzatto, L.; Hirono, A.; Beutler, E. Hematologically important mutations: Glucose-6-phosphate dehydrogenase. *Blood Cells Mol. Dis.* **1997**, *23*, 302–313. [[CrossRef](#)]
29. Minucci, A.; Giardina, B.; Zuppi, C.; Capoluongo, E. Glucose-6-phosphate dehydrogenase laboratory assay: How, when, and why? *IUBMB Life* **2009**, *61*, 27–34. [[CrossRef](#)] [[PubMed](#)]
30. Dalziel, K. Initial steady state velocities in the evaluation of enzyme-coenzyme-substrate reaction mechanisms. *Acta Chem. Scand.* **1957**, *11*, 1706–1723. [[CrossRef](#)]
31. Grabowska, D.; Jablonska-Skwiecinska, E.; Plochocka, D.; Chelstowska, A.; Lewandowska, I.; Witos, I.; Majewska, Z.; Rokicka-Milewska, R.; Burzynska, B. A novel mutation in the glucose-6-phosphate dehydrogenase gene in a subject with chronic nonspherocytic hemolytic anemia—Characterization of enzyme using yeast expression system and molecular modeling. *Blood Cells Mol. Dis.* **2004**, *32*, 124–130. [[CrossRef](#)] [[PubMed](#)]
32. Cunningham, A.D.; Colavin, A.; Huang, K.C.; Mochly-Rosen, D. Coupling between Protein Stability and Catalytic Activity Determines Pathogenicity of G6PD Variants. *Cell Rep.* **2017**, *18*, 2592–2599. [[CrossRef](#)] [[PubMed](#)]

33. Beutler, E. The genetics of glucose-6-phosphate dehydrogenase deficiency. *Semin. Hematol.* **1990**, *27*, 137–164. [[PubMed](#)]
34. Scopes, D.A.; Bautista, J.M.; Naylor, C.E.; Adams, M.J.; Mason, P.J. Amino acid substitutions at the dimer interface of human glucose-6-phosphate dehydrogenase that increase thermostability and reduce the stabilizing effect of NADP. *Eur. J. Biochem.* **1998**, *251*, 382–388. [[CrossRef](#)] [[PubMed](#)]
35. Verma, A.; Chandra, S.; Suthar, M.K.; Doharey, P.K.; Siddiqi, M.I.; Saxena, J.K. NADP<sup>+</sup> binding effects tryptophan accessibility, folding and stability of recombinant B. malayi G6PD. *Int. J. Biol. Macromol.* **2016**, *85*, 645–654. [[CrossRef](#)] [[PubMed](#)]
36. Gómez-Gallego, F.; Garrido-Pertierra, A.; Bautista, J.M. Structural Defects Underlying Protein Dysfunction in Human Glucose-6-phosphate Dehydrogenase A<sup>-</sup> Deficiency. *J. Biol. Chem.* **2000**, *275*, 9256–9262. [[CrossRef](#)] [[PubMed](#)]
37. Chotia, C. The Nature of the Accessible and Buried Surfaces in Proteins. *J. Mol. Biol.* **1976**, *105*, 1–12. [[CrossRef](#)]



© 2017 by the authors. Licensee MDPI, Basel, Switzerland. This article is an open access article distributed under the terms and conditions of the Creative Commons Attribution (CC BY) license (<http://creativecommons.org/licenses/by/4.0/>).